The baseline wander correction based on improved EEMD algorithm for grounded electrical source airborne transient electromagnetic signals

Yuan Li [1], Song Gao[2,3], Saimin Zhang[1,2], Hu He[3], Pengfei Xian[3], Chunmei Yuan[3]

[1]College of Geophysics, Chengdu University of Technology, Chengdu, 610059, China
[2]Key Laboratory of Earth Exploration and Information Techniques of Ministry of Education, Chengdu, 610059, China
[3]College of Information Science and Technology, Chengdu University of Technology, Chengdu, 610059, China

Correspondence to: Yuan Li (86210111@qq.com)

Abstract. The grounded electrical source airborne transient electromagnetic (GREATEM) system is an important method for obtaining subsurface conductivity distribution as well as outstanding detection efficiency and easy flight control. However, ~~the signals~~ there are the superposition of ~~useful~~ desired signals and various noise for GREATEM signal~~s~~. The baseline wander caused by the receiving coil motion always exists in the process of data acquisition to affect the measurement results. The baseline wander is one of the main noise sources ~~of data,~~ which has its own characteristics such as the low frequency, large amplitude, non-periodic and non-stationary and so on. Consequently, it is important to correction GREATEM signal ~~baseline wander~~ for inversion explanation ~~of GREATEM~~. In this paper, we propose improving method of EEMD by adaptive filtering (EEMD-AF)~~EEMD-AF~~ based on ensemble empirical mode decomposition (EEMD) to suppress~~correction~~ baseline wander. Firstly, the~~The~~ EEMD-AF method will decompose the electromagnetic signal into multi-stage intrinsic mode function (IMF) components. Subsequently, the ~~and~~ adaptive~~ly~~ filter will process higher index ~~high-order~~ IMF components ~~which~~ containing the baseline wander. Lastly, the de-noised signal will be reconstructed. To examine the performance of our introduced method, we processed the simulated and field signal containing the baseline wander by different methods. ~~we used the EEMD-AF method for the signal baseline correction and compared with sym8 wavelet with 10 decomposition levels and EEMD with deleted higher-order components directly. The various methods were applied to process the synthetic data and field data.~~ Through the evaluation of the signal-to-noise ratio (SNR) and mean-square-error (MSE), the ~~correction~~ result indicates that the signal using EEMD-AF method can get higher SNR and lower MSE. Comparing correctional data~~signal~~ using the EEMD-AF and the wavelet-based method in the anomaly curves profile images of the response signal, it is proved that the EEMD-AF method is a practical and effective method for suppression~~removal~~ of the baseline wander on GREATEM signal.

批注 [L1]: (1) Comments from Reviewer 2
(2) Author's response:
The grammatical and term errors in the paper will be corrected carefully.
(3) Author's changes:
The grammatical and term errors in this paper will be corrected carefully.

1 Introduction

The ~~grounded electrical source airborne transient electromagnetic (~~GREATEM~~)~~ system consists of two parts: the ground transmitter and air receiver system. This method takes advantage of the Airborne electromagnetic method (AEM) and the Magnetotelluric method (MT), which has large detection depth, higher signal resolution and outstanding detection efficiency (Mogi T,1998; Smith R S, 2001).

There are the superposition of desired signals and various noise for GREATEM signal. ~~The measured signals are the superposition of useful signals and various noise signals.~~ The noise may be divided into stationary white noise and non-stationary noise. According to the various noise source, the noise is usually classified as~~which contained~~ sferics noise, human electromagnetic noise and motion-induced noise (Abderrezak et al., 2010; Buselli et al., 1998; Macnae et al., 1984). The s~~S~~ferics noise is mainly caused by the charge discharge in the atmosphere, and the frequency is within 1k Hz. Human electromagnetic noise is caused by 50 Hz or 60 Hz industrial frequencies and its odd harmonics. Motion-induced noise comes from the receiving coil motion and has its own characteristics, such as low frequency, large amplitude, non-periodic and non-stationary. The signal baseline wanders caused by motion noise is one of the major interferences with the GREATEM signal. ~~The noise from the receiving coil motion is one of the major noises of the GREATEM signal, which could cause the baseline wander, resulting in signals with a dispersed, non-stationary and low frequency distribution.~~ This phenomenon always exists in the process of data acquisition to affect the measurement results. Severe baseline wander~~s in the measured EM signal~~ leads to inferior resistivity image formation and lower~~affect the~~ reliability of inversion explanation in the measured respond signal. After removing ~~sferics noise, human electromagnetic noise and motion-induced~~above noises, the processed data will be stacked and averaged on the next stage.

Because the ~~air~~ receiver system is mounted on aircraft such as the rotor-wing unmanned aerial vehicle (UAV) and airship, GREATEM system is different from AEM. First, during the flight, because the vibration and speed of the aircraft are weaker than airborne electromagnetic system ~~so that~~, the amplitude of the mounted coil swing is smaller. Hence, the fake anomalous amplitude of GREATEM caused by baseline wander is smaller than AEM ~~signals~~. Second, there is narrower frequency distribution ~~the frequency~~ of the baseline wander for GREATEM signal. ~~signal is narrower than airborne electromagnetic system.~~ The frequency distribution of the motion-induced noise ~~of the AEM~~ is within 1kHz for the AEM, while the frequency distribution of baseline~~range of GREATEM~~ is mostly within a few Hz for GREATEM in the actual measurement. Third, due to the use of miniaturized aircraft~~airship~~ ~~of~~ for GREATEM, the maximum flight loads are much less than the AEM. It is impossible to install the correctional complex mechanical structure to suppress baseline wander on the ~~receiving~~ receiver system ~~to filter out baseline wander~~. Therefore, it is necessary to develop the algorithm processing for the suppression of baseline wander.

In the method to suppress~~of filtering out~~ baseline wander, on the one hand mechanical correctional structure and hardware filter can be installed ~~increased~~, on the other hand digital filter~~ing~~ and fitting can be used for data processing. Some of studies ~~on the motion-induced noise~~ have focussed on the correctional method to suppress motion-induced noise on the transient electromagnetic system~~GREATEM signal~~. The Fugro company developed the time_~~-~~domain airborne electromagnetic system where the~~, which installed~~ hardware compensation devices ~~in the hardware to correct coil motion,~~ and ~~used~~ the notch filter with center frequency of 0.5Hz are installed to correct coil motion in the data acquisition system~~in the data processing~~. Buselli et al. (1998) proposed that ~~a~~ the high-pass filter with a cut-off frequency of 10Hz be used to reduce this noise~~to filter out coil motion~~. Lemire et al. (2001) raised ~~used~~ the spline interpolation and Lagrange optimization method to reject~~remove~~ low frequency noise. Yuan et al. (2013) introduced wavelet-based ~~for signal~~ baseline drift correction method using sym8 wavelet and 10 decomposition ~~with 10~~ layers. The wavelet-based method is based on multi-resolution decomposition analysis. But b~~B~~ecause it is difficult for wavelet decomposition to choose optimal wavelet basis function and ~~the~~ layer levels ~~of wavelet decomposition~~, ~~this~~ such methods ~~has~~ have poor adaptability. Patrick et al. (2004) raised the detrend method based on EEMD. This method consists of two steps. First, the trend be regarded as baseline estimate which be expected to be captured by IMFs of large index. Second, the reconstructed signal be amounted to the partial IMFs from lower index to middle index without the higher index components directly. Fubo et al. (2017) focussed on EEMD method to distinguish and suppress motion-induced noise in grounded electrical source airborne TEM system. Because the components containing motion-induced noise are excluded from the reconstructed signal directly, the reconstructed signal was distorted by these EEMD method.~~But this method distorted reconstructed signals by deleting the components with motion-induced noise directly.~~

N.E.Huang et al.(1998) proposed empirical mode decomposition (EMD) and Z. Wu et al.(2009) raised~~found~~ EEMD. The EMD and EEMD method is a scale-adaptive time-domain method which is applied to non-linear~~,~~ and non-stationary signal decomposition. For non-stationary signal processing, it is necessary~~demanded~~ to propose short time Fourier transform (STFT)~~STFT~~ and wavelet transform generally. The main method of STFT is to divide the signal into short time intervals where the signal is approximately stationary, and then perform the Fourier transform of signal on each time interval to get the frequency distribution. And the main method of the wavelet transform is to utilize a variable-scale sliding window where the specific data is approximately stationary on signal. The width of window is variable for time and frequency domain. However, because it is difficult to choose optimal wavelet basis function and the layer levels of wavelet decomposition by the signal itself, this method has poor adaptability. Therefore, ~~But~~ the requirement of signal characteristic above method is stationary in a specific window as same as the Fourier transform.

Different from previous methods, the major advantage of the EEMD is that the decomposition is derived from the signal itself. Therefore, the EEMD analysis is adaptive decomposition in contrast to the traditional methods ~~where~~ that the decomposition functions are fixed in a specific window throughout the processing. In addition,~~Finally,~~ the characteristics of the signal itself are not affected in the sifting process.

According to the characteristics of baseline wander for GREATEM signal, the EEMD ~~adaptive filtering (EEMD-AF) is presented in this paper. This~~ method consists of three steps.

step 1. The signal is decomposed into the N-level IMF components and the residual component by the EEMD method.

批注 [L2]: (1) Comments from Reviewer 1
(2) Author's response:
The authors update and check references.
(3) Author's changes:
The authors update and check references, and add two references from Section 3.2 by the removal of section 3.2.

批注 [L3]: (1) Comments from Reviewer 2
(2) Author's response:
The authors add section on the contrast of STFT and wavelet transform methods.
(3) Author's changes:
The contrast of STFT and wavelet transform method required signal is stationary in a specific window as same as the Fourier transform.
The EEMD is that the decomposition is derived from the signal itself in next section.

step 2. It is careful to use an adaptive~~a~~ low-pass filter for higher index~~high-order~~ IMFs to get ~~filter off~~ baseline wander estimate~~signal~~.

step 3. The de-noised~~noise-free~~ signal can be obtained by subtracting baseline wander from the noisy signal.

In the later section, compared with that of wavelet-based and EEMD without the higher index~~with deleted higher-order~~ components~~ directly~~, the correctional result shows that the EEMD-AF method is a practical and effective ~~method~~ for suppression~~removal~~ of the baseline wander on GREATEM signal.

2 Correction method of EEMD-AF

2.1 EMD methods

The ~~EMD method decomposes the~~ signal $S(t)$~~S(t)~~ is decomposed into N-level IMF components and a residual component by the EMD method. The EMD involves the adaptive decomposition of ~~gave~~ signal $S(t)$~~S(t)~~ by means of ~~a decomposition process called~~ the sifting process~~algorithm~~. The term of IMF is adopted because it represents the oscillation mode embedded in the data. The sifting process is defined by the following steps:

step 1. Identify levels of decomposition N, and $r_{j-1}(t) = S(t)$ ~~$r_{j-1}(t)=S(t)$~~ as residual parameter;

step 2. Extract IMF_j~~IMF_j~~;

(a) all extrema of $r_{j-1}(t)$~~$r_{j-1}(t)$~~;

(b) Interpolate local maxima and minima as the upper and lower envelopes separately by a cubic spline line. And compute "envelope" $E_{min}(t)$~~$Emin(t)$~~ and $E_{max}(t)$~~$Emax(t)$~~;

(c) Compute the average component $m(t) = (E_{min}(t) + E_{max}(t))/2$~~$m(t) = (Emin(t) + Emax(t))/2$~~;

(d) Extract the detail component $D_i(t) = x(t) - m(t)$;

(e) Iterate step (a) to step (d) on the detail component $D(t)$~~$D(t)$~~ until the stopping criterion satisfy threshold~~satisfy stopping criterion~~, $sd < \varepsilon$. Once criterion is achieved, the Detail $D(t)$~~$D(t)$~~ is considered as the effective IMF_j~~$IMF_j(t)$,~~ which also~~can~~ be considered as zero-mean generally. Calculate stopping criterion:

$$sd = \sum \frac{|D_{i-1}(t) - D_i(t)|^2}{D_{i-1}(t)^2} \tag{1}$$

step 3. Update residual: $r_j(t) = r_{j-1}(t) - IMF_j(t)$~~$r_j(t)=r_{j-1}(t) - IMF_j(t)$~~, the residual is deemed as the input for a new round of iterations;

step 4. Repeat step 2 and 3~~with j~~ until the value of j~~j~~ equal to N.

The stop criterion threshold ε ~~of the sifting process~~ is set between 0.2 to 0.3. The result of the sifting procedure is that S(t) will be decomposed into $IMF_j(t)$~~$IMF_j(t)$~~, $j = 1, \cdots, N$~~j = 1, …N~~ and residual $r_N(t)$~~$r_N(t)$~~.

$$S(t) = \sum_{j=1}^{N} IMF_j(t) + r_N(t) \tag{2}$$

2.2 EEMD methods

EEMD method is an improved method based on EMD~~ algorithm to eliminate the mode mixing problem of EMD~~ method. Compared with the EMD method, the EEMD method resolves the mode mixing problem and achieves better performance by adding white noise to the original signal (Z.Wu and N.E. Huang, 2004). For EEMD method, ~~The~~ the first step is to ~~EEMD~~ produces an ensemble of data-sets by adding finite amplitude σ~~different realizations~~ of ~~a~~ Gaussian distribution white noise ~~with finite amplitude σ~~ to the original data. The σ stands for ~~is~~ standard deviation of white noise. ~~The following,~~Then EMD method ~~repeated NE times~~ is applied to each realization of datasets ~~data series of the ensemble~~ to get $\mathrm{IMF_i(t)}$~~.~~ with NE times repeatedly. The next step is that the expected~~Finally, the~~ $\widehat{\mathrm{IMF}}_j$ is obtained by averaging the respective components in each realization to compensate for the effect of the addition ~~offset the impact~~ of the Gaussian white noise.

$$\widehat{\mathrm{IMF}}_j(t) = \frac{1}{NE}\sum_{i=1}^{NE} \mathrm{IMF}_i(t) \tag{3}$$

where NE is the ensemble numbers. Finally, the result of the sifting procedure is that S(t) will be decomposed into $\widehat{\mathrm{IMF}}_j(t)$, $j = 1, \cdots, N$~~j = 1, …N~~ and residual $r_N(t)$~~rN(t)~~.

$$S(t) = \sum_{j=1}^{N} \widehat{\mathrm{IMF}}_j(t) + r_N(t) \tag{4}$$

where σ is set between 0.05 to 0.2 and NE is set~~ to~~ between 100 to 400~~200~~. In this paper, we set σ and NE to 0.1 and 200 respectively.

2.3 EEMD-AF methods

The EEMD method is equivalent to a sifting filter~~,~~ which sifts out each IMF component ~~the~~ from signal $S(t)$~~S(t)~~ according to~~from fast~~ oscillations from fast to slow~~ oscillations for each IMF component~~. The lower~~-order~~ index IMF component mainly contains fast oscillations, meanwhile the higher~~-order~~ index IMF component mainly contains slow oscillations. The baseline wander is expected to be captured by higher~~-order~~ index IMFs~~ of large indices~~. The simple removal of several higher index ~~Simply removing the last several~~ IMFs may introduce significant distortions of ~~the~~ reconstructed signal. Thus, the baseline wander is distributed over the desired components in ~~the last~~ several higher index IMFs. To suppress ~~remove~~ the baseline wander, this method introduces a group of adaptive low-pass filter to process the ~~last~~ several higher index IMFs successively. The sum of the output of these filters is regarded as the reconstructed baseline estimate. Finally, the de-noised~~noise-free~~ signal can be obtained by subtracting an estimated baseline from the noisy signal.

First of all, we~~We~~ suppose the signal $S(t)$~~S(t)~~ contained severe baseline wander. After processing ~~the~~ by EEMD, $S(t)$~~S(t)~~ will be decomposed into IMFs which be referred to as~~ to~~ $a_k(t)$~~ak(t)~~:

$$S(t) = \sum_{k=1}^{N} a_k(t) \tag{5}$$

where N is the number of IMFs. Then, it is important to find out how much~~which number of~~ IMFs contribute~~s~~ to the baseline wander. Denote this number value as M. The $a_k(t)$~~ak(t)~~ is processed from the higher to lower index~~high-order to low-order~~ by low-pass filter of $h_k(t)$~~hk(t)~~. The output of ~~this~~ filter is $b_k(t)$~~ as:~~

$$b_k(t) = h_k(t) * a_k(t) \tag{6}$$

where $*$ denotes the convolution. The $h_k(t)$~~$h_k(t)$~~ is the Butterworth low-pass filter~~, and~~ whose ~~the~~ cut-off frequency is ω_k. As the IMF ~~order~~ index decreases, fewer slow oscillations components, but more signal components are contained in each IMF~~s~~. So, we design a group of adaptive low-pass filter ~~with~~ whose cut-off frequency be ~~decreases~~ decreased as IMF ~~order~~ index decreases. In other words, the first processing of filter is that the last IMF, $a_N(t)$, convolved with the first low-pass filter whose cut-off frequency is $\omega_N(t)$.~~The method processes the IMFs starting from the last, $a_N(t)$, filtered by first cut-off frequency $\omega_N(t)$.~~ And the~~The~~ cut-off frequency decreased along with the k index~~of the k-th~~ filter decreased~~is set as:~~.

$$\omega_{k-1} = \omega_k * \alpha \tag{7}$$

where α is set between 0.1 to 0.99 and $k = N, \cdots, 2, 1$. By this means ~~The~~ the filter output $b_k(t)$ contained low-frequency components are extracted from each IMF. Because the algorithm has to be adaptive,~~Next,~~ the output can be used to determine value of M as the condition of the reconstructed signal. According to analysis of procedure above~~the characteristics of IMFs~~, the amplitude of the baseline should gradually decrease as the IMFs index~~order~~ decreases on filter output $b_k(t)$. As a result, to determine the value of M, we consider using valuation coefficient function P_k~~take the standard deviation $std(b_k)$ from $b_k(t)$ and evaluation coefficient P_k regarded~~ as stopping criterion where the $std(b_k)$ stands for standard deviation b_k.

$$P_k = \frac{flip(std(b_k))}{\frac{1}{k-1}\sum_{i=1}^{k-1} flip(std(b_k))} \tag{8}$$

where $k = 1,2,\cdots,N$, The operator *flip* is the flipped function that the data rearrange in the opposite direction. The evaluation~~Set the threshold~~ coefficient threshold $\delta\varepsilon$ is set whose ~~and the~~ value range from 0 to 0.1. If $P_k < \delta\varepsilon$, the value~~the cut-off order~~ $M = N + 1 - k$. In this process, we set ω_N, α, ε to 10, 0.9 and 0.01~~,~~ respectively. The sum of output of filtered ~~filter-off~~ IMFs whose index is~~with orders~~ from M+1 to N is regarded as the reconstructed baseline estimate.

$$\widehat{b(t)} = \sum_{k=M+1}^{N} b_k(t) \tag{9}$$

Finally, to obtain reconstructed de-noised signal, the baseline estimate is subtracted from the original signal.

$$\widehat{S(t)} = S(t) - \widehat{b(t)} \tag{10}$$

3 Simulation data analysis

3.1 Simulation data

In GREATEM system, the transmitter injects a bipolar square wave current into the ground, meanwhile the receiver and front-mounted coil were installed on an aircraft to response to the vertical component of the induced electromotive force in a horizontal layered earth model (Nabighian et al, 1988). Responded signals are related to the size and depth of the underground conductor, the~~ line~~ length and current of the transmitter, the equivalent area of the receiving coil, the horizontal offset, the flight altitude and so on. These parameters can be used to calculate the time domain response as clean signal in the horizontal layer earth model for simulation. In Fig. 1, the model parameters~~ are~~ as follow~~s~~: the length of the transmitter line

TX is 1000 m on the ground, the transmitter current ~~I~~ is 10 A with 50% duty cycles at 25 Hz ~~a frequency of 25Hz~~, the equivalent area of ~~the~~ receiving coil RX is 1000 m^2, the horizontal offset ~~location of receiver~~ is 50 m, the flight altitude is 35 m, the sample rate of receiver is 32k Hz. In this paper, we consider three−layer earth model where parameters are shown in Table 1. In the end, we calculated the corresponding time domain signal and the vertical response decay curve ~~and the corresponding time domain signal~~ on a three-layer earth model.

Because of non-periodic and non-stationary characteristics of baseline wander, it is difficult to synthesize these~~this~~ noise from simulation on the computer. The simulated~~synthetic~~ signal is obtained by superimposing the clean signal on the field baseline wander measured by the inertial navigation system ~~to clean signal system~~. Fig. 2(a) is simulated~~synthetic~~ noisy signal which is obtained by adding baseline wander to clean signal with the duration is 10 ~~second~~s. Fig. 2(b) is the field baseline wander noise which is measured by the inertial navigation system with the duration is 10 s~~with 10 seconds~~.

~~3.2 Other methods of correction~~

~~3.2.1 EEMD correction~~

~~In the EEMD method, the trend regarded as baseline estimate is expected to be captured by IMFs of large order. The reconstructed signal may therefore amount to the partial IMFs from lower-order to middle-order with ignored higher-order components directly (Patrick Flandrin et al., 2004).~~

~~3.2.2 Wavelet-based correction~~

~~The wavelet-based method is based on multi-resolution decomposition analysis, which can employ commonly used wavelet bases (e.g. Haar, db2, db4, db8, sym2, sym4, sym8) with 8 to 12 decomposition levels in processing data. After comparing result, the optimal wavelet basis is sym8, and the decomposition level is 10 (Yuan et al., 2013).~~

批注 [L4]: (1) Comments from Reviewer 2
(2) Author's response:
Section 3.2 describe the other method for subsequent analysis. Section 3.2.1 and 3.2.2 statement will be combined and added to specific referenced papers on Section Introduction.
(3) Author's changes:
The content of section 3.2 extracted and changed to Section Introduction as reference.

3.~~3~~ 2 Performance of the correction and analysis

In this paper, in order to quantitatively assess the de-noised~~detrending~~ quality between our method and other methods, we propose the signal-to-noise ratio (SNR) and mean square error (MSE) to evaluate the correctional~~correction~~ methods ~~quantitatively~~ in ~~equation~~ Equation 11 and 12, in which S(n) is synthetic clean signal, $\widehat{S(n)}$ is de-noised~~processed~~ signal, L is the number~~length~~ of samples. The higher the SNR, the better the correctional effect; the lower the MSE, the better the fitting result. ~~There are comparison of the SNR and MSE of the synthetic noisy signal on before and after correction using EEMD-AF, wavelet-based and EEMD method, respectively.~~

$$\mathrm{SNR} = 10\lg\left(\frac{\sum_{n=1}^{L} S^2(n)}{\sum_{n=1}^{L}(S(n)-\widehat{S(n)})^2}\right) \tag{11}$$

$$\mathrm{MSE} = \frac{\sum_{n=1}^{L}(S(n)-\widehat{S(n)})^2}{L} \tag{12}$$

There are comparison of the SNR and MSE before and after correction using EEMD-AF, wavelet-based method with sym8 and level 10, and EEMD method with ignored higher index IMFs directly. Through the noisy signal of duration of 60 s is processed by three methods the correctional results are shown in Table 2. ~~In Table 2, the correctional result of noisy signal with 60 seconds applied by three methods are shown,~~ in which the term Noisy signal means simulated ~~SNR of synthetic~~ noisy signal before correction. The SNR value shows that the three methods have a remarkable improvement in signal quality. It is proved that EEMD-AF and wavelet-based method had better correctional performance than EEMD. Quantitatively, SNR of EEMD-AF method ~~yields SNR, which~~ is significantly close to SNR achieved by the wavelet-based method. It is obvious ~~It can be shown~~ that the EEMD-AF achieves correction performance as similar to the wavelet-based method.

For further analysis,~~ in the data processing of GREATEM system,~~ the response decay curve is related to the conductivity of underground geological bodies in the data processing of GREATEM. Besides the ~~above~~ SNR comparison above~~on time domain signal~~, the original~~processed~~ data~~ above~~ are used for stacking, averaging and extracting secondary field to build one by one test point along with ~~on~~ the ~~whole~~ survey path. Then the number of time gates are 24 on per test point where the width of time gates increases ~~the gates are~~ approximately logarithmically. ~~spaced by 24 gates per point. Generally, the gates were referred to as channels.~~

To generate the anomaly curves profile image, we process the simulated~~synthetic~~ noisy data and correctional data by stacking, averaging, extracting and gating.~~using EEMD-AF and wavelet-based method.~~ The anomaly curves profile generated from the clean signal responses ~~are~~ is shown in Fig. 3(a), where ~~represented~~ the 24 paralleled line of time gates were represented~~24 channels~~ along with the test point. And the Fig. 3(b) is anomaly curves profile generated from the ~~calculated~~ noisy signal~~ responses~~, where ~~we can clearly identify~~ the fake anomaly from ~~Channel~~ Gate 14 to ~~end~~ 24 is identified clearly due to baseline wander affected ~~the interference of baseline wander on~~ the horizontal earth model. From the ~~Channel~~ Gate 20 to 24, they mixed each other. After the processing using the wavelet-based method, the anomaly curves profile is shown in Fig. 3(c), where the fake anomaly is not accurately represented and the curves are similar to parallel each other. Fig. 3(d) is the anomaly curves profile using the EEMD-AF method, it is pretty obvious that the paralleled curves between the gates~~channels~~ are better than the above method.

The~~A typical~~ comparison of SNR and MSE profile produced by the datasets on different method ~~different method~~ is illustrated ~~along with the test point~~ in Fig. 4 along with the test point, where SNR and MSE of the noisy signal ~~is~~ are marked as reference (black solid curve~~line~~). In Fig. 4(a), the black solid curve~~the processing of noisy signal~~ shows that the stacking and averaging may produce the improved SNR for noisy signal. Quantitatively, the EEMD-AF and wavelet-based method yields SNR~~,~~ which is significantly higher than value achieved by the EEMD method. It is observed that there are fluctuations of SNR using wavelet-based method (blue solid curve~~line~~) meanwhile there are stabilities of SNR using EEMD-AF method (red solid curve~~line~~). And in Fig. 4(b), the MSE curves indicate~~s~~ the same conclusion. Results from the comparison of the figures~~both methods~~ also show that the EEMD-AF ~~correctional~~ method significantly outperforms the wavelet-based for the suppression of non-stationary baseline wander.

4. Field data analysis

In October 2018, an field experimental GREATEM survey had been~~was~~ performed to detect infiltration water in the refuse landfill of Longquanyi District, Chengdu in China. The GREATEM system was developed by Chengdu University of Technology. The electrical source transmitter was fixed on the ground meanwhile the receiver system ~~is~~ was mounted on the six rotor UAV. The survey area and flight paths of the receiver~~GREATEM system~~ ~~is~~ were shown in Fig. 5(b). The length of the transmitter line was 1100 m on the ground, the transmitter waveform was bipolar square wave~~,~~ and ~~transmitter~~ current was 20 A with 50% duty cycles at 5 Hz. The receiver system made use of 24-bit Analog-to-Digital Converter ~~and~~ whose sample rate was 32k Hz~~,~~ and the equivalent area of the receiving coil ~~is~~ was 1000 m^2. The transmitter line was set in the middle of flight paths and almost perpendicular to ~~each other~~them. ~~The~~ Each length of the flight ~~line~~ path was 800 m and the intervals were~~spacing was~~ 80 m each other. The flight speed of the UAV was 2.5 m/s~~,~~ and the ~~flight~~ height ~~was~~ were 50 m from the ground~~surface~~.

The amplitude of the response will decrease with the ~~increase of~~ transmitter–receiver offset increase. We choose measured data of part of flight path L4 for our processed, and the duration~~data of length~~ of 60 ~~second~~s of data ~~are~~ is shown in Fig. 6(a). ~~We can significantly observe the~~The baseline wander is observed on the measured data significantly~~signal~~. And Fig. 6(b) is the correction result from the EEMD-AF method. By ~~visual~~ comparison of the ~~data~~ signals before and after processing, the baseline wander is effectively suppressed ~~eliminated~~ by EEMD-AF method.

Besides the ~~above visual~~ comparison of time domain data above, we produced anomaly curves profile image ~~of~~ from the original measured data~~,~~ and the correctional data which is processed ~~the corrected data with~~by the wavelet-based method and the EEMD-AF method~~,~~ respectively. The number of time gates is 18 and the widths are increase approximately logarithmically on per test point. ~~The gates are approximately logarithmically spaced with 18 gates referred to as 18 channels per point.~~ Fig. 7(a) ~~is~~ shows the anomaly curves profile generated from the measured raw data~~,~~. The~~Fig. 7(b) is the~~ correctional data using the wavelet-based and ~~Fig. 7(c) using the~~ EEMD-AF method are shown on Fig. 7(b) and (c) respectively~~correction~~. Based on the survey area ~~are~~ for refuse landfill, ~~we know that~~ the geological structure can be considered as~~of the flight area is~~ layered earth, ~~that~~ there may be partial regions where the infiltration water was leaked.

~~Therefore, in~~In Fig. 7(a), the higher amplitude of responded anomaly curves reflected at 220 m, 270 m and 300 m in the flight survey ~~line~~path.~~,~~ Therefore, the baseline wander exists in the original signal so as to ~~which will~~ affect exploration elevation and the anomalies result on inversion ~~because of the baseline wander existing in the original signal~~. It is obvious to observe the fake anomalies from the ~~Channel~~ Gate 10 to 15 and the interference~~interfere~~ with each other from the Gate~~Channel~~ 16 to 18. In Fig. 7(b) and (c), after using ~~the baseline~~two correction methods, the fake anomalies are suppressed~~reduced~~ ~~from~~ on the ~~Channel~~ Gate 10 to 15, and it is improved to interfere with each other from the Gate~~Channel~~ 16 to 18. In addition, ~~The~~ the Fig.7(c) shows that there is no interference between the Gates. However, ~~the channels while~~ there is partial interference on the Gate~~Channel~~ 16 to 18 ~~especially~~ in Fig.7(b). Contrast with wavelet-based method, there is no interference between last three channels for datasets using EEMD-AF method on anomaly curves profile. For that the decay time of curves, the EEMD-AF method hold decay time 4.5 milliseconds more than wavelet-based method to improve the exploration elevation on the survey path. Comparison of Fig. 7(b) and (c), the results reveal that the performance of EEMD-AF method is significantly superior to the wavelet-based method to suppress~~remove out~~ baseline wander. In a word, the results confirm EEMD-AF method is an effective and~~,~~ practical correctional method.

5 Conclusion

Motion-induced noise was usually referred to as baseline wander ~~that~~ which is an inevitable noise and always exists for GREATEM system. The noise caused by the receiving coil motion has its own characteristics such as~~with~~ low frequency, large amplitude, non-periodic and non-stationary. This phenomenon affects ~~The noise is caused by the receiving coil motion and always exists in the process of data acquisition to affect~~ the accuracy of measurement ~~results~~ severely, leading to the inferior ~~the~~ exploration elevation and the fake anomalies result on inversion. Therefore, we proposed the improved EEMD-AF~~EEMD~~ method for baseline wander correction. The noisy signal is decomposed into N-level IMF components and residual component by EEMD method, and the baseline wander is generally distributed over in several higher index~~the desired components in the last several~~ IMFs, then a group of adaptive low-pass filter process ~~last several~~these IMFs successively. The baseline estimate~~sum of the filter output~~ is reconstructed by the sum of these filter output~~as a baseline estimate~~. Finally, the de-noised~~noise-free~~ signal can be obtained by subtracting an estimated baseline wander from the noisy signal.

First of all,~~In this paper,~~ through comparison of different de-noised method in this paper~~synthetic noisy data using correctional method of EEMD, wavelet-based and EEMD-AF~~, the SNR and MSE results show that the de-noised performance of EEMD-AF method ~~performance~~ is significantly superior to the other methods. And~~Furthermore,~~ the same conclusion can be reached ~~for~~ from the anomaly curves profile image. Furthermore,~~When processing~~ in field data processed, the baseline wander is effectively suppressed by EEMD-AF and wavelet-based methods. Because there is no interference between the last few Gates. ~~However,~~ the ~~results of~~ comparison of the anomaly curves profile image reveals that EEMD-AF method is significantly better than~~superior to~~ the wavelet-based method ~~to remove out baseline wander~~. ~~Contrast with wavelet-based method, there is no interference between last three channels for data using EEMD-AF method on anomaly curves profile. And the decay curves of the whole survey line hold decay time 4.5ms more than wavelet-based method to improve the exploration elevation.~~ These results also indicate that the EEMD-AF~~improved EEMD~~ method is a practical as well as effective method for the suppression~~removal~~ of the baseline wander on GREATEM signal.

批注 [L5]: (1) Comments from Reviewer 1 and 2
(2) Author's response:
The authors revise the 'conclusions' section and get solid conclusion, some discussion will be added to the 'Field data analysis'.
(3) Author's changes:
The 'conclusions' section is revised and some discussion will be added to the 'Field data analysis'.

Data availability

In this paper, the data are not publicly accessible~~,~~ because funder terms require to kept confidential for the original geological data without cooperative licensing agreements.

Author contribution

First, Yuan L. and Song G. designed the method model and developed code. Second, ~~The~~ the author Saimin Z. designed the field experiments and carried it out with Hu H. and Pengfei X. on survey area. Third, Yuan L. and Chunmei Y. performed the simulations and processed data. Finally, Yuan L. prepared the manuscript with contributions from all co-authors.

Competing interests

There are no competing interests in this paper. And the authors declare that they have no conflict of interest.

Acknowledgements

This study was carried out within the project '~~supported by~~ Research on fixed wing time domain airborne electromagnetic measurement technology system (2017YFC0601904)' supported by the Institute of Geophysical and Geochemical Exploration, Chinese Academy of Geological Sciences. The authors thank the members of the project committee for their help.

References

Abderrezak, B., Micheal, C., Pierre, K., Richard, S.: Sferics noise reduction in time-domain electromagnetic systems: application to MegaTEM II signal enhancement, Explor. Geophys., 41, 225–239, doi:10.1071/EG09007, 2010.

Buselli, G., Hwang, H.S., Pik, P.J.: AEM noise reduction with remote referencing, Explor. Geophys., 29, 71–76, doi:10.1071/EG998071, 1998.

Blanco-Velasco M, Weng BW, Barner KE.: ECG signal denoising and baseline wander correction based on the empirical mode decomposition, Comput. Biol. Med., 38, 1–13, doi:10.1016/j.compbiomed.2007.06.003, 2008.

Macnae, J.C., Lamontagne, Y.,West, G.F.: Noise processing techniques for time-domain EM system, Geophysics, 49, 934–948, doi:10.1190/1.1826986, 1984.

Fubo L.，Jutao L.，Lihua L.: Application of the EEMD method for distinction and suppression of motion-induced noise in grounded electrical source airborne TEM system, J. Appl. Geophy., 139, 109-116, doi:10.1016/j.jappgeo.2017.02.013, 2017.

Lemire, D.: Baseline asymmetry, Tau projection, B-field estimation and automatic halfcycle rejection. Technical Report, THEM Geophysics Inc, 2001.

Mogi, T., Tanaka, Y., Kusunoki, K., Morikawa, T., and Jomori, N.: Development of grounded electrical source airborne transient EM(GREATEM), Explor. Geophys., 29, 61–64, doi:10.1071/EG998061, 1998.

Nabighian, M.N.: Electromagnetic methods in applied geophysics, Volume 1: Theory. Soc. Explor. Geophys., doi:10.1007/bf01452955, 1988.

N.E. Huang, Z. Shen, S.R. Long, M.C. Wu, H.H. Shin, Q. Zheng, N.C. Yen, C.C. Tung and H.H. Liu: The Empirical Mode Decomposition and the Hilbert spectrum for nonlinear and non-stationary time series analysis, Proc. Royal Soc. London A, vol. 454, 903-995, doi:10.1098/rspa.1998.0193, 1998.

P. Flandrin, P. Goncalves, G. Rilling: Detrending and denoising with empirical mode decomposition, 12th European Signal Processing Conference, Vienna, Austria, September 2004.

Smith, R. S., Annan, A. P., and McGowan, P. D.: A comparison of data from airborne, semi-airborne and ground electromagnetic systems, Geophysics, 66, 1379-1385, doi:10.1190/1.1487084, 2001.

Wang, Y., Ji, Y.J., Li, S.Y., et al.: A wavelet-based baseline drift correction method for grounded electrical source airborne transient electromagnetic signals, Explor. Geophys., 44, 229-237, doi:10.1071/EG12078, 2013.

Z. Wu, N.E. Huang.: Ensemble empirical mode decomposition: a noise-assisted data analysis method, Adv. Adapt. Data Anal, 1, 1-41, doi:10.1142/S1793536909000047, 2009.

Z. Wu, N.E. Huang.: A study of the characteristics of white noise using the empirical mode decomposition method, Proc. R. Soc. A 460 (2046), 1597–1611, doi:10.1098/rspa.2003.1221, 2004.

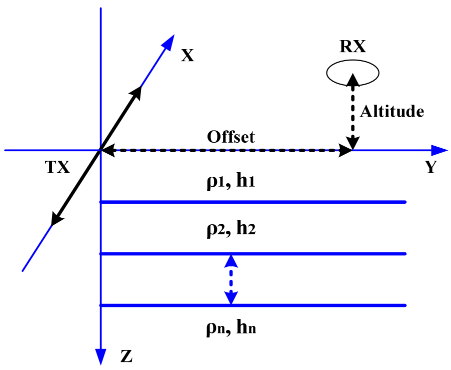

Figure 1: GREATEM model based on three-layer earth model. **The TX is the transmitter line on the ground and the line length is 1000 m, the transmitter current is 10 A and frequency is 25 Hz. The RX is receiving coil and the equivalent area is 1000 m², the offset is 50 m, the flight altitude is 35 m, the sample rate of receiver is 32k Hz. The other model ~~where~~ parameters are shown in Table 1.**

批注 [L6]: (1) Comments from Reviewer 1 and 2
(2) Author's response:
The authors updated description of figure 1, 3, 5, 7 in accordance with manuscript. The interpretation of figure contains more details.
(3) Author's changes:
The description of figure contains more details for interpretation.

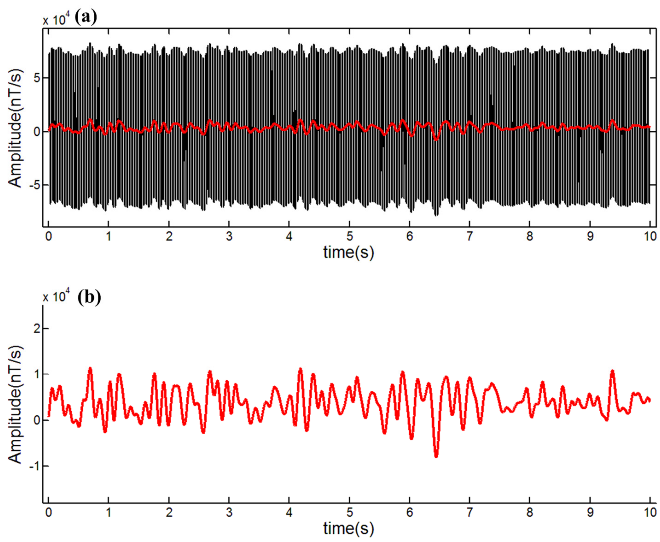

Figure 2: The simulated~~synthetic~~ noisy signal and baseline wander signal whose duration is 10 s. (a) The simulated~~synthetic~~ noisy signals; (b) the field baseline wander measured by the inertial navigation system.

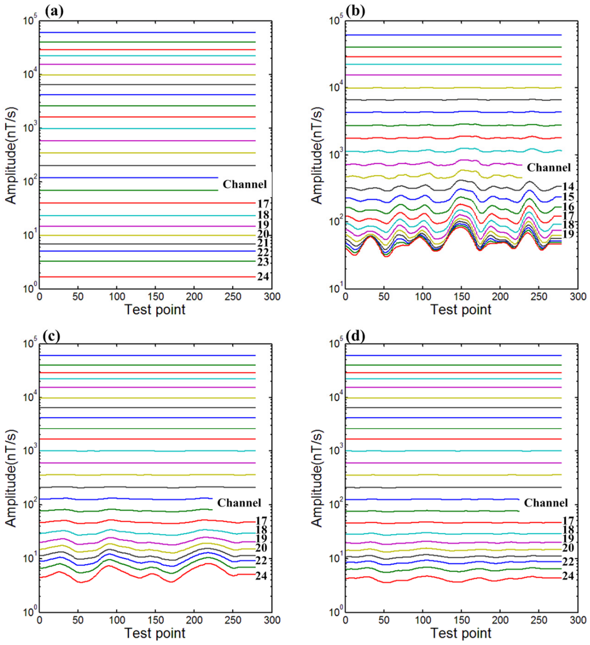
(a)
(b)
(c)
(d)
Amplitude(nT/s)
Test point
Channel
14
15
16
17
18
19
20
21
22
23
24

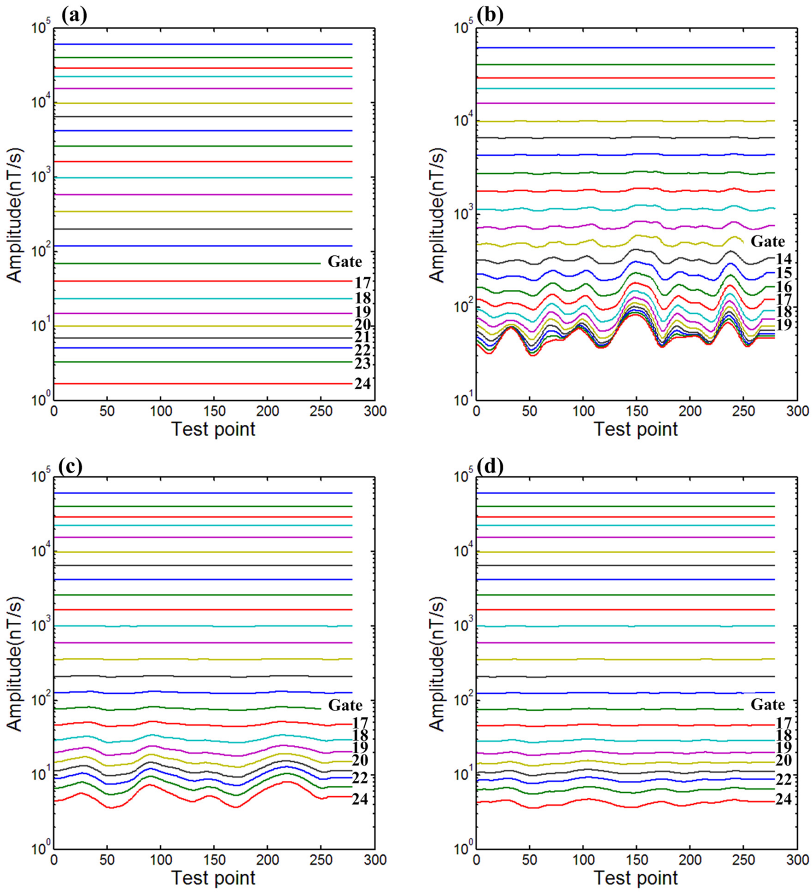

Figure 3: Anomaly curves profile image generated from different processed datasets.~~:~~ The duration of raw data is 60 s and the stacking interval is 0.2 s therefore the number of Test points is 300. (a) The clean signal from the theoretical model; (b) the noisy signal containing baseline wander; (c) the correctional signal~~data~~ using wavelet-based method; (d) the correctional signal~~data~~ using EEMD-AF method. The label Gate marked in each figure represents the number of time gates from 1 to 24. Every specific number of time gate means different time width which increased logarithmically.

批注 [L7]: (1) Comments from Reviewer 1 and 2
(2) Author's response:
The authors updated description of figure 1, 3, 5, 7 in accordance with manuscript. The interpretation of figure contains more details.
(3) Author's changes:
The description of figure contains more details for interpretation.

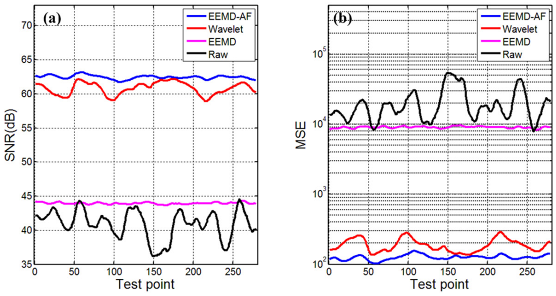

Figure 4: Comparison of SNR and MSE profile produced by datasets on the different methods ~~along with test point~~. (a) The contrast of SNR ~~of~~ on different datasets~~methods along with test point~~; (b) the contrast of MSE ~~of~~ on different datasets.~~different methods along with the test point.~~

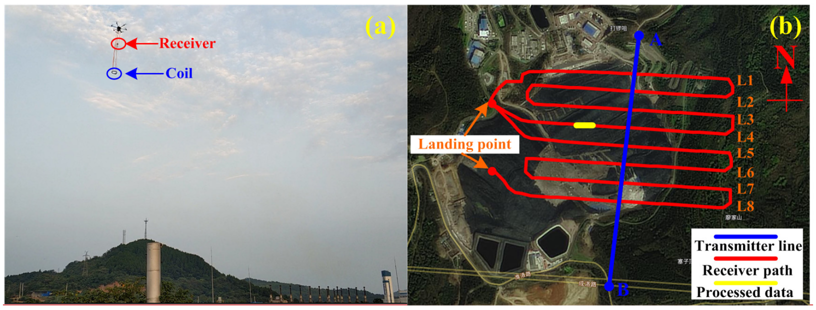

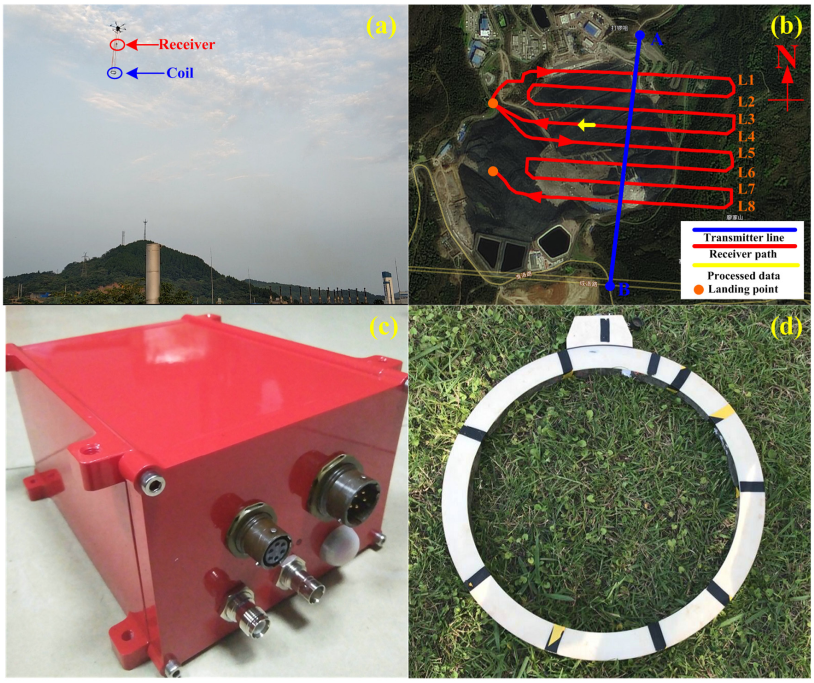

Figure 5: The survey area and flight paths on the refuse landfill of Longquanyi District, Chengdu in China~~of the GREATEM system~~. (a) The receiver system is mounted on UAV along with the paths~~.~~; (b) ~~The~~ the blue line was the transmitter source and the red ~~line~~ curves were ~~was~~ the survey paths of the receiver~~,~~; the lines of L1 through L8 represent different paths and the orange dots represent the landing point for UAV; (c) the receiver instruments; (d) the receiving coil with diameter of 50 cm. The flight heading was from east to west on the L4 path. The data of part of L4 (yellow arrow solid line) ~~was~~ will be processed and the duration ~~length of time~~ was 60 s~~econds~~. ~~(b) embedded the~~The satellite images embedded in figure (b) came from https://map.tianditu.gov.cn/ built by the National Geomatics Center of China.

带格式的: 正文

批注 [L8]: (1) Comments from Reviewer 1 and 2
(2) Author's response:
The authors updated description of figure 1, 3, 5, 7 in accordance with manuscript. The interpretation of figure contains more details.
(3) Author's changes:
The description of figure contains more details for interpretation.

批注 [L9]: (1) Comments from Reviewer 2
(2) Author's response:
The receiver instruments will be showed on Fig 5 (c) and (d).
(3) Author's changes:
The receiver instruments will be showed on Fig 5 (c) and (d). And the description of figure contains more details for interpretation.

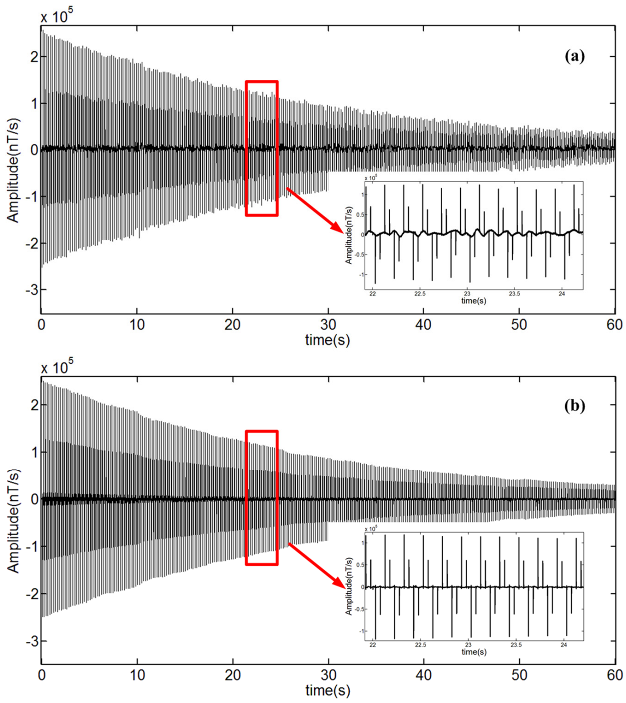

Figure 6: The ~~F~~field data whose duration is ~~with~~ 60 s~~econds~~ containing~~are plotted by~~ baseline wander and correctional data filtered by ~~signal using~~ the EEMD-AF method. (a) The field~~Field~~ data measured ~~acquisition~~ by receiver~~GREATEM~~ instruments; (b) the ~~corrected~~ correctional data ~~signal~~ using the EEMD-AF method. The data of 22 s to 24 s~~The signal~~ is magnified ~~from 22 seconds to 24 seconds~~ and shown at the lower right of each figure~~scheme~~.

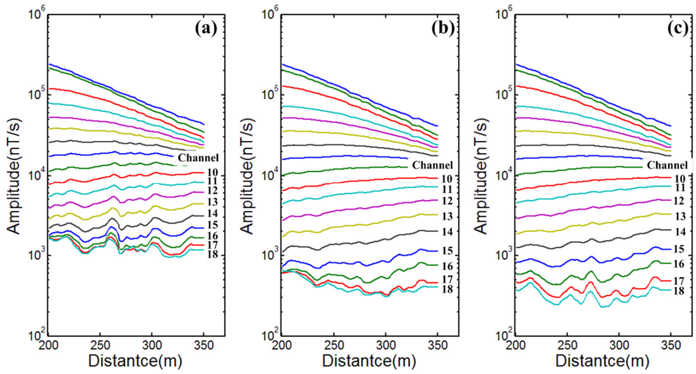

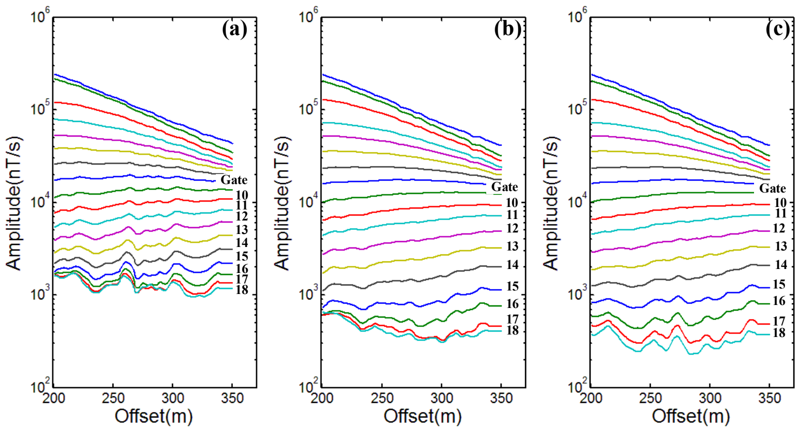

Figure 7: Anomaly curves profile image generated from field data on different methods.: (a) The ~~Profile~~ profile of raw data.; (b) the profile of data using wavelet-based method; (c) the profile of data using EEMD-AF method. Because the duration of raw data was 60 s and the flight speed of the UAV was 2.5 m/s, the offset distance was 150 m.

域代码已更改

批注 [L10]: (1) Comments from Reviewer 1 and 2
(2) Author's response:
The authors updated description of figure 1, 3, 5, 7 in accordance with manuscript. The interpretation of figure contains more details.
(3) Author's changes:
The description of figure contains more details for interpretation.

Table 1: Parameters of the three-layer earth model

Parameter	Resistivity ρ_n (Ω m)	Thickness h_n (m)
1st	150	100
2nd	30	100
3th	300	

Table 2 Correctional result comparison of SNR of different methods

Method	SNR(dB)
Noisy signal	5.0810
EEMD-AF	48.1462
EEMD	35.1025
Wavelet-based	48.2513